

International Journal of Energy Economics and Policy

ISSN: 2146-4553

available at http: www.econjournals.com

International Journal of Energy Economics and Policy, 2026, 16(6), 137-156.

Rice Husk Power Generation Potential in Casanare, Colombia: A Production-to-Mill Spatial Assessment

Julian E. Guerrero-Macias[1,2]*, Yecid A. Muñoz-Maldonado[1], Melitza M. Medina-Medina[1], Sylvia J. Sierra-Carrillo[1]

[1]Grupo de Investigación en Energía y Medio Ambiente (GIRES), Faculty of Engineering, Universidad Autónoma de Bucaramanga (UNAB), Bucaramanga, Santander, Colombia, [2]Grupo de Investigación en Ingeniería Civil para Ciudades Seguras y Sostenibles (INSECUS), Civil Engineering Program, Universidad Internacional del Trópico Americano (Unitrópico), Yopal, Casanare, Colombia. *Email: jguerrero9@unab.edu.co

Received: 24 June 2026 **Accepted:** 05 October 2026 **DOI:** https://doi.org/10.32479/ijeep.24724

ABSTRACT

Colombian energy planning increasingly treats residual biomass as a resource to be mobilised through territorial infrastructure, yet the national biomass inventory that still anchors regional estimates rests on agricultural data from 2006 -roughly two decades old- and departmental tonnage figures cannot indicate where a residue is generated or how much remains available for energy use. This study estimates the rice-husk electricity potential of Casanare, Colombia's leading paddy producer, through a spatially explicit and updatable framework based primarily on public data and calibrated against primary weighbridge records from one mill. A four-level traceability chain separates origin-based theoretical potential, milling-based generation, availability-adjusted potential, and technical electricity potential. Municipal paddy production is allocated to a verified inventory of milling nodes through an attractiveness-weighted spatial-interaction model, with nearest-neighbour and pure-distance specifications retained as structural bounds. Under the central parameter set, the gross technical electricity potential is 24.3 GWh/year (a mean output of 2.78 MW) with a spatial band of 19.0-32.5 GWh/year and an interannual band of 20.6-26.9 GWh/year. The assessment also finds that the mill-level data needed to validate such estimates are already collected under existing reporting obligations but are not publicly available in aggregate.

Keywords: Rice Husk, Biomass Energy, Spatial Allocation, Residual Biomass, Energy Policy
JEL Classification: Q42, Q48, O13, R58

1. INTRODUCTION

Colombia's energy planning increasingly treats residual biomass as a resource to be mobilised through territorial infrastructure rather than as a diffuse environmental externality. The current National Energy Plan proposes establishing a network of regional Bio-Hubs to promote the energy use of residual biomass and states the intention of integrating those regional hubs into the National Interconnected System (SIN) under distributed-generation or self-generation arrangements (UPME, 2025a). This is a specific planning commitment: It locates residual biomass not at the margins of the electricity system but as a candidate contributor to it, organised around regional concentrations of agro-industrial activity. Translating that commitment into project-level decisions requires knowing how much residue is actually generated, where it is physically concentrated, and how much of it is available after competing uses are accounted for. Aggregate departmental tonnages do not answer those questions.

Casanare illustrates both the opportunity and the informational obstacle. The department is Colombia's leading paddy producer, with a 2025 output of 1,224,167 t of green paddy (DANE et al., 2026), and rice husk is separated from the grain at industrial mills rather than left in the field. Unlike straw, husk is therefore a point-

This Journal is licensed under a Creative Commons Attribution 4.0 International License

source residue: It accumulates at a small number of identifiable facilities, which makes it comparatively tractable for energy conversion. The department also exhibits a pronounced internal disparity in electricity access. Reported urban coverage reaches 100%, while rural coverage stands at 78.26%, leaving an estimated 10,925 rural dwellings without service (UPME, 2025c). The access deficit in Casanare is thus not a departmental average problem but a rural distribution problem.

The plausible destination for this resource has recently changed. The Casanare-Vichada interconnection was commissioned in stages between May 2022 and March 2023, integrating a formerly non-interconnected area — including the rice-producing municipalities of Trinidad and San Luis de Palenque — into the National Interconnected System; in February 2023 the national agency for non-interconnected zones (IPSE) ceased monitoring Bocas de Pauto and Santa Rosalía as non-interconnected zones (XM, 2023; IPSE, 2023). Both municipalities are among the department's principal rice-producing areas. This interconnection reframes the question that a resource assessment should answer. Where isolated supply once implied evaluating husk as fuel for stand-alone systems, the relevant question now is whether the resource can contribute to the interconnected system in a region that retains a substantial rural access gap. Localities that remain isolated are typically small and remote, and supplying them with husk would require a transport and logistics assessment that lies beyond the scope of this study.

Estimating that contribution requires distinguishing between quantities that are routinely conflated. Municipal paddy production is an agricultural statistic; husk generation is an agro-industrial outcome determined by where grain is milled; husk availability depends on competing uses; and electricity potential depends further on moisture, heating value and conversion efficiency. Collapsing these into a single coefficient produces figures that cannot be audited or updated. The intermediate step is also the least observable: No Colombian public dataset reports the flow of paddy from producing municipalities to individual mills, nor verified throughput for each facility. That flow must therefore be modelled rather than measured, and the modelling assumptions must be declared explicitly.

This article addresses that gap through a spatially explicit and updatable assessment of rice-husk electricity potential in Casanare, based primarily on public data and calibrated against an aggregated primary dataset from one mill. The estimates are organised as a four-level traceability chain — origin-based theoretical potential, milling-based generation, availability-adjusted potential, and technical electricity potential — so that the attrition between the gross resource and the convertible resource remains visible at each step. The departmental figure reported by ENAM for 2025 establishes the scale of the resource; the estimates reported here are computed on the 2023 Fifth National Rice Census, which is the most recent source providing municipal disaggregation.

The contribution is twofold. Methodologically, the article demonstrates that a defensible municipality-to-mill allocation can be constructed from public registry, road-network and capacity evidence, with an explicit hierarchy governing which facilities enter the model and on what evidentiary basis. Empirically and for policy, it documents a reporting paradox: Several of the variables required to improve such an assessment are already subject to mandatory reporting under Colombian regulation, yet no aggregated public dataset derived from them is available. Departmental science and technology planning identifies rice-husk valorisation for energy as a priority (Gob Casanare, 2015), while the national coverage-expansion instrument does not develop a corresponding pathway for residual biomass (UPME, 2025b). The remainder of the article is organised as follows: Section 2 reviews the relevant literature, Section 3 details the data and methods, Section 4 reports the results, and Sections 5 and 6 discuss implications and conclude.

2. LITERATURE REVIEW AND BACKGROUND

This section reviews the literature required to connect agricultural production, rice milling, residual-biomass availability, and electricity generation within a spatially explicit assessment. It is organised around four questions: How residual-biomass potential is assessed spatially, what governs rice-husk generation and conversion, how spatial allocation can be modelled when flows are unobserved, and what the Colombian evidence and policy framework establish.

2.1. Residual Biomass Potential Assessment and GIS

Agricultural-residue assessments are most informative when they distinguish resource generation from resource availability. Production statistics and residue coefficients yield a gross potential, whereas the fraction actually collectable depends on competing uses, collection efficiency and the spatial configuration of supply. Chauhan (2010) formalised this distinction for Indian crop residues — separating generated, surplus and net-available biomass — showing that treating gross generation as an energy resource systematically overstates what is convertible. GIS-based studies extend this accounting by assigning quantities to explicit locations and linking them to infrastructure and candidate facilities; Siegrist et al. (2022) showed that techno-spatial restrictions materially reduce theoretical potentials once terrain, accessibility and plant-scale constraints are imposed. Availability is also time-dependent: Kongchouy et al. (2021) combined crop calendars, residue distributions and collection-factor scenarios to estimate seasonal power potential, demonstrating that annual totals conceal the temporal concentration that determines whether continuous generation is feasible. What remains less developed is the agro-industrial step in which a field residue becomes a point-source residue at a processing facility.

2.2. Rice Husk Generation, Fuel Properties and Energy Conversion

Rice-husk potential begins with a mass-balance problem. Husk is commonly reported as approximately 20% of paddy mass, but the applicability of that ratio depends on the paddy basis, milling configuration and variety. Because paddy is reported in Colombia on a green basis while husk ratios are typically defined on dry

paddy, applying a coefficient without declaring its basis introduces a systematic error propagating through every subsequent step. The energy content is likewise not a universal constant: Experimental characterisation reports dry-basis lower heating values between 13.24 and 16.20 MJ/kg alongside storage-dependent moisture (Mansaray and Ghaly, 1997; Wu et al., 2009), while silica-rich ash, low bulk density and non-uniform flow constrain technology selection. Natarajan et al. (1998) found fluidized-bed systems promising for husk combustion and gasification while identifying agglomeration limits, and Olupot et al. (2016) showed that husk characteristics differ enough between varieties to affect gasifier performance. Availability at the mill must be considered separately from generation: Kapur et al. (1996) demonstrated that a substantial share of husk may already be committed to internal thermal uses before any surplus becomes available. The literature thus provides defensible parameter ranges and confirms technical feasibility at mill scale, but not a method for determining how much paddy — and therefore husk — arrives at any particular mill.

2.3. Spatial Allocation and Interaction Models

The allocation problem is conceptually distinct from biomass quantification. Location-allocation models typically identify facility locations or assign demand under an optimisation criterion; the problem here is the inverse, since the facilities already exist and the unobserved quantity is the flow between origins and destinations. Bojesen et al. (2014) provide the central bioenergy antecedent by combining location allocation with a production-constrained spatial-interaction model, treating biomass supply as spatially competed rather than exclusively assigned — the relevant structure when several facilities draw from overlapping supply areas. Subsequent models added spatial and economic restrictions: Route optimisation and clustering for distributed rural bioenergy (Laasasenaho et al., 2019), network analysis with multi-criteria plant attributes (Ferrari et al., 2022), and two-phase GIS and location-allocation approaches for community-scale supply chains (Boonman et al., 2025). Food-flow research broadens the empirical basis where traceability is incomplete: Calibrated gravity models improve source reconstruction when shipment records are unavailable (Schlaich et al., 2020), distance, node size and accessibility jointly structure urban sourcing (Karg et al., 2025), and spatial-interaction models with balance constraints estimate subnational cereal flows (Jain, 2026).

The analogy with paddy allocation must be stated carefully. A rice mill does not demand paddy because of its attractiveness as an energy destination; it processes grain for commercial, logistical and contractual reasons. Interaction weights should therefore be read as a reference allocation consistent with observable attributes, not a behavioural model of procurement, and results should be bracketed by structural alternatives rather than presented as a single estimate. The remaining gap is an application to an existing paddy-milling system in which flows are unobserved, and facility capacity is only partially documented.

2.4. Agro-Industrial Residues and Grid-Connected Generation in Latin America

A distinct body of Latin American work evaluates agro-industrial residues not as fuel for isolated systems but as a source of surplus electricity delivered to national grids. Brazilian sugarcane research is the most developed case: Fioranelli and Bizzo (2023) identified the technological, contractual and logistical constraints that reduce realisable surplus below technical estimates; De Souza et al. (2021) distinguished gross from environmentally available potential by incorporating straw-removal limits; Bressanin et al. (2021) showed that surplus electricity is sensitive to the incentive framework rather than technical potential alone; and Furtado et al. (2023) addressed seasonality directly, modelling a hybrid plant combining vinasse biogas with surplus bagasse to extend annual operation.

Colombian work has followed a similar trajectory for oil palm. Montoya et al. (2020) evaluated surplus electricity and levelised costs across conversion configurations, and Barrera Hernández et al. (2024) constructed scenarios for twenty-eight plants accounting for existing energy systems and residue uses. That accounting matters: National inventory data show that mesocarp fibre and kernel shell are largely consumed in the mills' own boilers, while empty fruit bunches are predominantly returned to plantations (Ramírez Contreras et al., 2015), so palm residues carry well-established competing uses that must be discounted when estimating net availability. At national scale, Sagastume Gutiérrez et al. (2020) inventoried Colombian agricultural, agro-industrial and livestock residues, adopting available rather than gross residue as the accounting basis.

This literature establishes the framing adopted here — residues as a contributor to grid-connected supply, with availability constrained by existing uses — but concentrates on sugarcane and oil palm, where processing facilities are large, few and often already equipped with cogeneration. Rice milling differs on each count: Mills are more numerous, individually smaller and generally lack installed generation capacity, so the location of the resource relative to producing areas becomes a determinant of the estimate rather than a secondary consideration.

2.5. Colombian Context, Data Availability and Study Positioning

Colombian evidence confirms the scale of the rice-husk resource but remains fragmented across national inventories, agricultural statistics and plant-level experiments. The national Biomass Atlas (UPME et al., 2010) is one of the few departmental-scale antecedents, and its rice-husk residue factor of 0.20 has propagated through subsequent regional estimates; that inventory, however, draws its agricultural base from 2006 production data and compiles federation-supplied coefficients rather than primary determinations. More recent national academic estimates exist (Pérez-Rodríguez et al., 2022), but none institutionally replaces it or reproduces its departmental disaggregation — which motivates a framework designed to be re-run as newer public data become available. At the conversion stage, Lenis Rodas et al. (2022) demonstrated fixed-bed gasification of Colombian husk in compact mills, while Jyothsna et al. (2024) proposed intersectoral use through existing industrial infrastructure where individual mills are too small to justify dedicated generation.

Husk in Colombia is not a costless residue. Departmental planning records its use as a soil amendment and drying fuel within mills (Colciencias et al., 2012), and Colombian evidence documents established non-energy uses as a growing medium in nurseries, hydroponics and commercial floriculture, formally recognised in ICA Resolution 780006 of 2020, with reports of declining availability attributed to diversifying competing uses (Monsalve Camacho et al., 2021). A prior regional assessment additionally reports compacted husk supplying livestock-transport and feed markets, such that acquiring it entails a cost (Medina Medina and Sierra Carrillo, 2022). No public record was found of sector-wide consumption volumes or a reference market price, so availability is treated here as a declared scenario parameter rather than an estimated quantity.

The institutional framework reinforces the relevance of origin-destination information while exposing a data gap. Production sites and processing facilities are subject to registration (ICA, 2022), and mills, traders and agro-industrial actors must report monthly to SIRIARROZ - including volumes traded and storage capacity — under the monitored-freedom price regime regime (MADR, 2025, as amended by MADR, 2026), yet no aggregated public dataset derived from that obligation is available. The pattern recurs in industrial statistics, where the Annual Manufacturing Survey records husk consumed as an energy input and its allocation to self-generation and cogeneration (DANE, 2024) without publishing a corresponding aggregate. Departmental planning prioritises husk valorisation for energy (Gob Casanare, 2015), while the national coverage-expansion plan does not develop a specific pathway for residual biomass (UPME, 2025b).

Taken together, the most developed spatial bioenergy applications are concentrated in Europe and Asia; the Latin American grid-connected residue literature centres on sugarcane and oil palm; and the Colombian rice-husk literature is national and aggregate or experimental at plant scale. No published assessment connects municipal paddy production, allocation to identified mills, husk generation, availability under competing uses, and technical electricity potential for a Colombian department. This study addresses that gap for Casanare and documents the reporting asymmetry that prevents such assessments from being validated against observed flows.

3. MATERIALS AND METHODS

This section describes a replicable, spatially explicit and updatable procedure based primarily on public data, complemented by one primary weighbridge dataset used as the calibration anchor. Figure 1 summarizes the full mass-energy flow, and Tables 1-5 document the data sources, mill inventory and evidence hierarchy, attractiveness scoring, allocation models and parameter scenarios, respectively. Extended justifications, declared-but-unexecuted specifications and robustness details are provided in the Supplementary Material (S1–S8) and referenced at the relevant points below.

The chain proceeds from municipal green paddy production to gross technical electricity potential. Level 2 operates under two allocation regimes: An exogenous capacity regime, deducted before competitive allocation, and an attractiveness-weighted competitive regime calibrated against primary weighbridge data. Conversion follows a biomass gasification power generation (BGPG) reference pathway.

Figure 1: Four-level mass-energy traceability chain

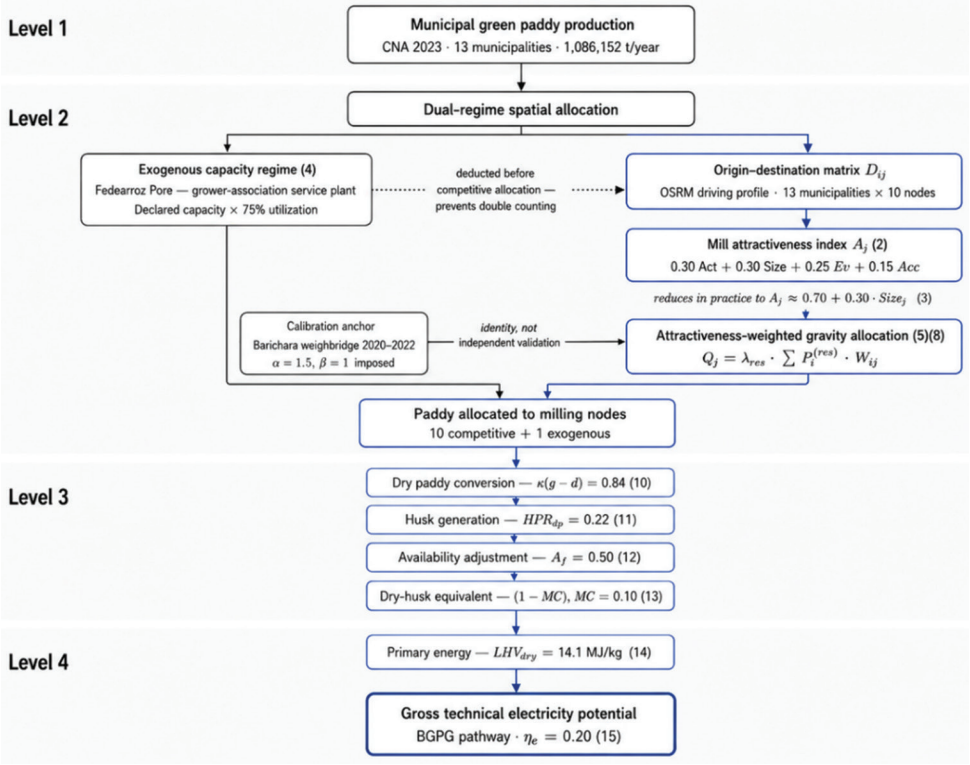


Table 1: Data sources and methodological variables used in the rice husk potential assessment

Level	Variable	Description	Primary source (s)
Level 1	$P_{i,t}$	Municipal green paddy production (t/year)	CNA 2023 (base, executed); EVA 2024 (cross-source robustness); ENAM 2025 (departmental anchor, declared not executed)
Level 1	κg-d=0.84	Green-to-dry paddy conversion coefficient	DANE (2014), rice agro-industry satellite account
Level 2	M_j	Public inventory of milling nodes	RUES/Chamber of Commerce (CIIU 1051); OSM/Google Maps; ICA Res. 00004706/2022; Durán Hernández et al. (2021); corporate and press sources
Level 2	D_{ij}	Municipality-mill road-network distance	OSRM driving profile (Luxen and Vetter, 2011) over OpenStreetMap (OpenStreetMap contributors, 2026)
Level 2	A_j	Public mill attractiveness index (Act, Size, Ev, Acc)	RUES; storage-capacity evidence hierarchy [Table 2]; routed road network
Level 2	λ_res, λ_eff	Residual and effective local-processing fractions	Calibrated against Molino Barichara weighbridge records (2020-2022)
Level 2	HPRdp	Husk-to-paddy ratio, dry-paddy basis (0.22 central)	UPRA (2020), Table 26, p. 111; UPME et al. (2010), Annex E, Table 29, p. 163; Barichara weighbridge (22.1%)
Level 3	*Af*	Availability factor (0.25/0.50/0.75/1.00)	Scenario design (this study), contextualized by Kapur et al. (1996)
Level 3	MC	Moisture content, wet basis (0.08/0.10/0.15)	Mansaray and Ghaly (1997); Olupot et al. (2016); Wu et al. (2009)
Level 3	LHVdry	Lower heating value, dry basis (13.2/14.1/16.2 MJ/kg)	Mansaray and Ghaly (1997); Wu et al. (2009)
Level 4	η_e	BGPG electrical conversion efficiency (0.20 central; 0.25 high)	Wu et al. (2009); study-defined reference

HPRdp is a husk-generation coefficient on a dry-paddy basis; the dry-husk equivalent is obtained via the MC term in Equation (11). η_e is a BGPG-specific scenario parameter. Results are reported as gross technical electricity potential

Table 2: Evidence hierarchy for mill storage capacity and consequences for model inclusion

Tier	Evidence class	Consequence for the model	Nodes assigned
1	Primary measured data (weighbridge records)	Included; capacity taken as measured	Arroz Barichara (6,300 t)
2	Plant-specific corporate or press source	Included; capacity taken as reported, material basis declared	Arrocera La Esmeralda (65,000 t; Grupo Empresarial Blanquita, 2024); Unión de Arroceros (40,000 t; Prensa Libre Casanare, 2022); Molinos El Yopal (30,000 t, dry-paddy basis; Molinos El Yopal S.A.S., n.d.)
3	Regional survey applied uniformly (Durán Hernández et al., 2021)	Included; applied to *every* node lacking a more specific source	ORF Pore; ORF Villanueva; Agroindustrial Sonora (100,000 t each); Diana Corporación; Granos y Cereales de Colombia (80,000 t each)
4	Size-class regression imputation	Included with reduced Act_j=0.5	Molino Casanare (8,570 t)
5	No capacity documented after exhaustive audit (sixteen source categories)	Excluded from the capacity-weighted specification; retained in the distance-only robustness test	Molinos Agroindustrial del Casanare
—	Institutional exclusion (non-market service plant)	Removed from competitive allocation; incorporated through the exogenous capacity regime (Section 3.5)	Fedearroz-Pore

Tier 3 capacities are 2018 regional-survey estimates attributed by the source to its own compilation; this provenance limitation is carried into the Limitations section. Tier 2 figures are reported by the companies without a uniformly declared material basis; the consequence for the La Esmeralda node is quantified in Section 4.9. The Tier 5 audit covered sixteen source categories (commercial registry, equipment suppliers, import records, environmental files by tax identification number, financial directories, corporate networks and direct contact)

Table 3: Scoring rules for the mill attractiveness index components

Component	Definition	Scoring rule	Source
Act_j	Legal/registration status	Active and renewed=1; operational currency partially verified=0.5; inactive=0	RUES/Chamber of Commerce
$Size_j$	Storage capacity	Continuous min-max normalization across competitive nodes	Evidence hierarchy, Table 2
Ev_j	Evidence of recent operation	Verified operation=1; indirect evidence=0.5; none=0	web/OSM/Google/manual
Acc_j	Road accessibility	1 if node lies within 250 m of the routed road network	OSM road network

All components are normalized to 0-1 before aggregation in Equation (2)

3.1. Study Area and Assessment Architecture

The study area is the department of Casanare, in the Eastern Plains (Llanos Orientales) of Colombia, one of the country's leading paddy-producing regions. The assessment focuses on rice husk rather than rice straw because husk is a point-source agro-industrial residue concentrated at mills during dehusking, whereas straw remains spatially diffuse across harvested fields; this concentration makes husk both easier to inventory and more realistic to convert into energy at identifiable facilities.

Table 4: Spatial allocation models: Assumptions, role and anchoring references

Model	Assumption	Role	Anchoring references
M1 Nearest-neighbour	All municipal paddy to the single nearest node	Lower dispersion bound	Laasasenaho et al. (2019); Singlitico et al. (2019)
M2 Pure gravity	Flow ∝ inverse distance; no heterogeneity	Structural sensitivity	Schlaich et al. (2020); Bojesen et al. (2014); Karg et al. (2025); Jain (2026)
M3 Attractiveness-weighted gravity	Flow ∝ attractiveness and inverse distance	Reference specification	Bojesen et al. (2014); Ferrari et al. (2022); Boonman et al. (2025); Siegrist et al. (2022)

All three models operate on the residual pool net of the exogenous deduction, apply λ_res uniformly, and use (D_{ij}+ε) to prevent division by zero

Table 5: Parameters, scenarios and evidence basis

Parameter	Value/scenarios	Unit	Basis	Role	Source and exact location
P^{CNA}	1,086,152	t/year	Green paddy	Executed base	DANE et al. (2024), CNA 2023, Cuadro 33 (13 municipalities)
P^{ENAM}	1,224,167	t/year	Green paddy	Declared, not executed	DANE et al. (2026), Table 10, departmental row
κg-d	0.84	t/t	Green→dry	Central	DANE (2014), rice satellite account
HPRdp	0.22 (range 0.18-0.25)	t/t	Dry paddy	Central	UPRA (2020), Table 26, p. 111; corroborated by Barichara weighbridge (22.1%)
HPRdp (antecedent)	0.20	t/t	Residue/product	Regional antecedent; lower reference	UPME et al. (2010), Annex E, Table 29, p. 163
α	1.5	—	Distance friction	Imposed structurally	Not estimated; single-anchor identification limit
β	1.0	—	Attractiveness elasticity	Imposed structurally	Not estimated; single-anchor identification limit
λ_res	Calibrated	frac.	Residual pool	Calibrated+two bands	Barichara weighbridge (2020-2022)
λ_eff	Reported outcome	frac.	Departmental	Derived	Model output
Fedearroz utilization	0.75	frac.	Capacity	Exogenous regime	Federación Nacional de Arroceros (2015)
Af	0.25/0.50/0.75/1.00	frac.	Scenario	Central 0.50	This study; contextualized by Kapur et al. (1996)
MC	0.08/0.10/0.15	frac.	Wet basis	Sensitivity	Mansaray and Ghaly (1997); Olupot et al. (2016); Wu et al. (2009)
LHVdry	13.2/14.1/16.2	MJ/kg	Dry basis	Sensitivity	Mansaray and Ghaly (1997); Wu et al. (2009, 14.14 MJ/kg)
η_e	0.20/0.25	frac.	BGPG	Central/high	Wu et al. (2009), p. 591 (25%)
η_e (bounds)	0.10/0.30	frac.	BGPG	Context only	Olupot et al. (2016); Wu et al. (2009), 5.5-MW system
δaux	0.15	frac.	Auxiliary loads	Net adjustment	Olupot et al. (2016)

Bold entries denote the central specification. Results are reported as gross technical electricity potential unless δaux is explicitly applied

The methodology is organized as a four-level traceability chain that separates the agricultural, agro-industrial, physical-generation and energy dimensions of the resource rather than collapsing them into a single tonnage figure: (i) origin-based theoretical rice husk potential; (ii) regional milling-based rice husk generation potential; (iii) availability-adjusted rice husk potential; and (iv) technical electricity generation potential. Each level is reported separately in the Results so that the attrition between the theoretical resource and the technically convertible resource remains visible. A defining feature of the approach is that the second level — the transfer of paddy from producing municipalities to milling nodes — is not observable in Colombia from public records; it is therefore modeled rather than measured, and every quantity downstream of that step is reported as model-implied and conditional on the inventory and calibration assumptions declared below.

3.2. Data Sources and Preprocessing

The municipal agricultural base is characterized through the variable $P_{i,t}$, the green (freshly harvested) paddy production of municipality i in year t (t/year). The primary municipal distribution is derived from the Quinto Censo Nacional Arrocero (CNA; Fifth National Rice Census) because it is crop-specific and census-based (DANE et al., 2024); the Evaluaciones Agropecuarias Municipales (EVA) dataset is used as a cross-source robustness specification (UPRA, 2024). All quantitative results reported in this article are computed on the CNA 2023 base (13 rice-producing municipalities; 1,086,152 t of green paddy). A spatial-stability check between CNA 2023 and EVA 2024 is reported in Section 4.1.

Green paddy is converted to dry paddy through the coefficient κg-d = 0.84, the wet-to-dry conversion coefficient reported in DANE's rice agro-industry satellite account (DANE, 2014), which operates on paddy mass and is independent of the husk moisture correction applied later. All data sources are consolidated in Table 1, with parameter values and their evidence basis detailed in Table 5.

For years in which only a departmental figure exists - such as the 2025 ENAM total of 1,224,167 t for Casanare (DANE et al., 2026) - a share-preserving scaling specification is declared to keep the procedure updatable. That specification is declared for reproducibility only and is not applied to the results reported here, which are computed directly on the CNA 2023 municipal distribution; it is documented in Supplementary Material S1, together with the reason a 2025 departmental anchor is not mixed with a 2023 municipal distribution and a 2020-2022 calibration window.

3.3. Rice Mill Inventory and Evidence Hierarchy for Capacity

The set of milling nodes operating in Casanare is denoted M_j. Legal status is taken from RUES and Chamber of Commerce records (RUES, 2026), with the CIIU code (1051) used as an eligibility criterion rather than an index component; geolocation is obtained from OpenStreetMap and Google Maps; and operational status is confirmed through web-based evidence and manual verification, following the institutional definition of a rice mill in ICA Resolution No. 00004706 of 2022 (ICA, 2022). Because storage capacity is the only observable that discriminates among nodes in the attractiveness index (Section 3.4), the evidence supporting each capacity figure determines both whether a node enters the model and with what weight. A single evidence hierarchy is therefore declared and applied uniformly, so that inclusion follows from a stated rule rather than case-by-case judgement; nodes are assigned to the highest tier for which a source exists (Table 2).

Two properties govern the results. Tier 3 is applied uniformly by construction: Once Durán Hernández et al. (2021) is admitted for any node, consistency requires admitting it for every node lacking a higher-tier source. And absence of a documented capacity is treated as a public-information gap rather than zero capacity, so the single Tier 5 node is excluded from the reference specification and bounded through the distance-only specification of Section 3.8 (Supplementary Material S2).

Primary field data were obtained from one node (Molino Barichara, km 8 on the Yopal-Aguazul road), which provided individual weighbridge records for 2020-2022 together with husk percentage by silo (observed husk fraction 22.1%). Annual throughputs were reconstructed from the individual weighing entries rather than from summary-sheet totals, which contained running-accumulator artifacts. These data serve two distinct functions, kept separate throughout: Corroboration of an intensive parameter (HPRdp, Section 3.6) and calibration of an extensive one (λ, Section 3.6).

3.4. Spatial Structure: Distance Matrix and Attractiveness Index

3.4.1. Origin-destination matrix

The spatial relationship between producing municipalities and mills is captured by the matrix D_{ij}, defined as the fastest-route road distance returned by the OSRM `driving` profile over OpenStreetMap road data (Luxen and Vetter, 2011; OpenStreetMap contributors, 2026). Because the `driving` profile optimizes travel time rather than geometric path length, the returned distance is not in general the shortest-path distance; this is stated because it affects reproducibility. The matrix comprises 13 municipalities ×10 competitive nodes = 130 origin-destination pairs, plus 13 additional pairs for the exogenous-regime deduction of Section 3.5. Municipal seats were used as production-proxy points because publicly georeferenced paddy-plot data were not available at the required scale, a limitation acknowledged in Section 5. A backward-compatibility control against the original eight-node matrix is reported in Supplementary Material S3. The resulting spatial configuration is mapped in Figure 2; no spatial operation is performed on the map, and all allocation is computed on D_{ij}.

3.4.2. Attractiveness index

Mill heterogeneity is represented by a public attractiveness index A_j, built from four observable components normalized to a 0-1 scale before aggregation (Table 3):

$$A_j = 0.30 \cdot Act_j + 0.30 \cdot Size_j + 0.25 \cdot Ev_j + 0.15 \cdot Acc_j \quad (2)$$

Where Act_j is legal/registration status, $Size_j$ a normalized storage-capacity proxy, Ev_j evidence of recent operation, and Acc_j road accessibility. A rice-proximity term was deliberately excluded to avoid double penalization of distance, already captured through D_{ij}. Two specification details are declared: $Size_j$ is a continuous min-max normalization of storage capacity rather than a discrete size-class score, because a categorical rule assigned nearly all nodes an identical score and made the attractiveness-weighted model numerically indistinguishable from pure gravity (S3); and Acc_j = 1.0 for all nodes, since every node lies within 250 m of the routed road network, so accessibility functions as a binary connectivity condition that all nodes satisfy.

Because Act_j, Ev_j and Acc_j saturate at their maxima for all nodes but one, Equation (2) reduces in practice to

$$A_j \approx 0.70 + 0.30 \cdot Size_j \quad (3)$$

So that the specification is, under the available public evidence, more precisely a storage-informed gravity model than a fully discriminating multi-criteria index. The four-component structure is retained because it makes this saturation visible and because the non-saturating components would discriminate given richer registry data; the empirical content of A_j is concentrated in the capacity evidence of Table 2 (see S2).

3.5. Dual-Regime Spatial Allocation

Paddy is allocated to milling nodes under two distinct regimes, because the inventory contains one node whose institutional nature is incompatible with market-competitive allocation.

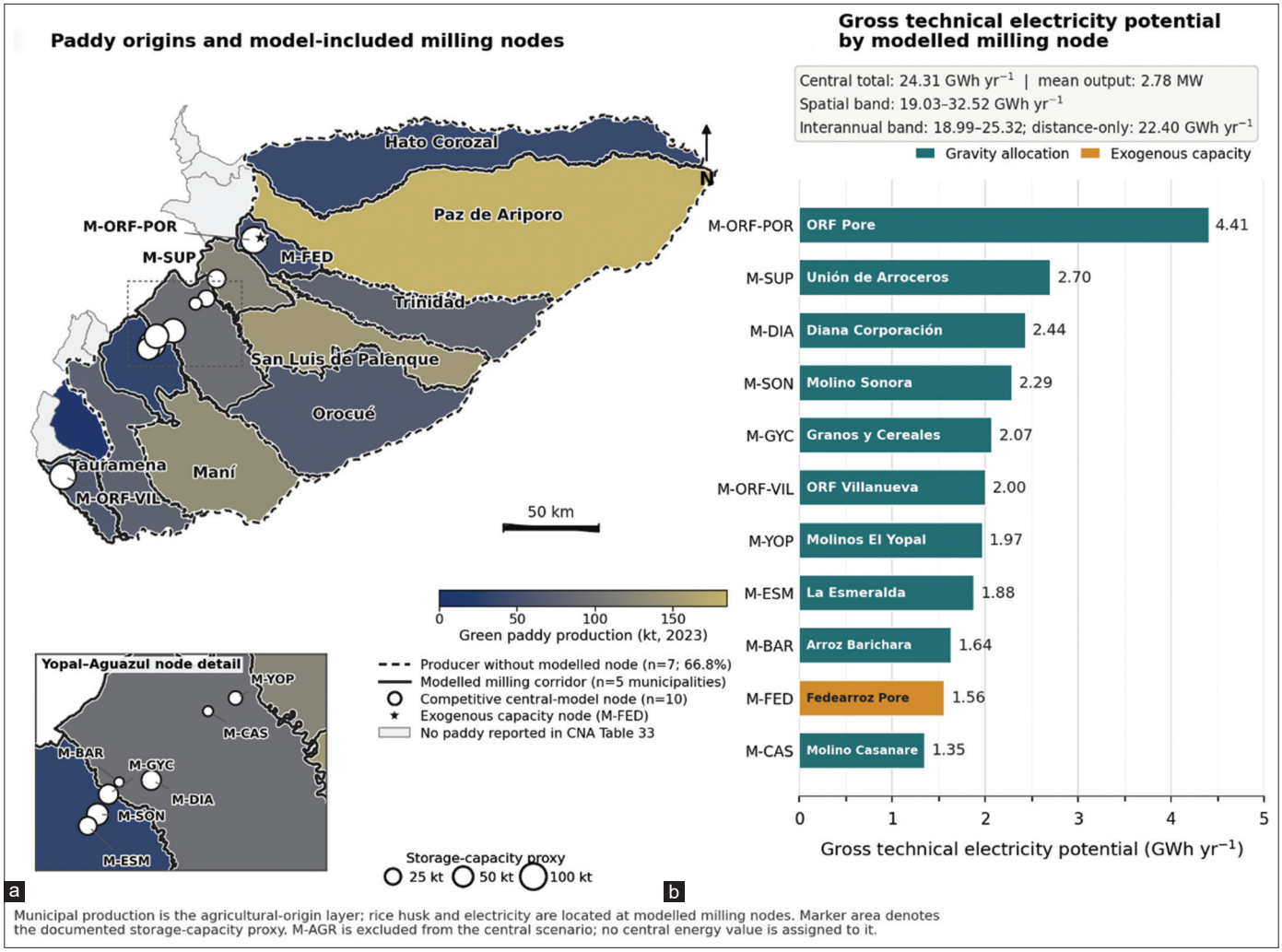
3.5.1. Exogenous capacity regime

The Fedearroz plant at Pore is a grower-association (*gremial*) service facility milling on behalf of affiliated growers rather than purchasing paddy on the open market (Federación Nacional de Arroceros, n.d.), so its throughput is estimated exogenously. Applying a 75% utilisation factor to its documented capacity of 2,240 t of dry paddy per month (26,880 t/year; Federación Nacional de Arroceros, 2015) gives an annual intake converted to a green-paddy basis through κg-d:

$$Q^{exo}_Fedearroz = (2{,}240 \times 12 \times 0.75)/\kappa_\{g\text{-}d\} \quad (4)$$

This intake is deducted from municipal production before competitive allocation proceeds, concentrated in the municipalities nearest the plant (Pore supplying 97.7% of it). The deduction prevents the same paddy from being counted once through the exogenous regime and again through the competitive weights.

Figure 2: Spatial separation between paddy origins, milling infrastructure and modelled rice-husk electricity potential in Casanare. (a) Municipal green-paddy production (CNA 2023) and the eleven milling nodes included in the central model; marker area denotes the documented storage-capacity proxy, and node codes correspond to panel (b). Dashed outline: Seven producing municipalities without a modelled node (66.8% of departmental paddy). Solid outline: The five-municipality milling corridor. The inset resolves the overlapping Yopal–Aguazul nodes. (b) Gross technical electricity potential by node under the central scenario; the ten competitive nodes are allocated through the attractiveness-weighted gravity regime, whereas M-FED is incorporated through the exogenous capacity regime. Bars sum to 24.3 GWh yr^{-1}. The capacity-undocumented node evaluated only in the distance-only robustness specification is not assigned a central-scenario value.



Municipal production is the agricultural-origin layer; rice husk and electricity are located at modelled milling nodes. Marker area denotes the documented storage-capacity proxy. M-AGR is excluded from the central scenario; no central energy value is assigned to it.

3.5.2. Competitive regime

The remaining ten nodes compete for the residual municipal pool through three allocation specifications of increasing structural richness (Table 4), sharing the common form

$$Q^{green}_\{j,t\} = \lambda_res\ \Sigma_i\ P^{res}_\{i,t\}\ W_\{ij\} \quad (5)$$

Where $P^{res}_{i,t}$ is municipal production net of the exogenous deduction and λ_res is the residual local-processing fraction calibrated in Section 3.6. A small positive constant ε is added to D_{ij} to prevent division by zero where a mill lies within its origin municipality. The three specifications are:

$$Model\ 1\ (nearest):\ Q^N_\{j,t\} = \lambda_res \cdot \Sigma_i\ P^{res}_\{i,t\} \cdot I(j = nearest(i)) \quad (6)$$

$$Model\ 2\ (gravity):\ W^D_\{ij\} = (D_\{ij\}+\varepsilon)^{-a} / \Sigma_j\ (D_\{ij\}+\varepsilon)^{-a} \quad (7)$$

$$Model\ 3\ (weighted):\ W^G_\{ij\} = A_j^{\beta}(D_\{ij\}+\varepsilon)^{-a} / \Sigma_j\ A_j^{\beta}(D_\{ij\}+\varepsilon)^{-a} \quad (8)$$

Model 1 assigns all municipal paddy to the nearest node, serving as the lower bound of spatial dispersion (Laasasenaho et al., 2019; Singlitico et al., 2019); Model 2 distributes flow by distance decay while ignoring mill heterogeneity (Schlaich et al., 2020; Bojesen et al., 2014); and Model 3, which makes flow depend jointly on distance and attractiveness, is adopted as the reference specification because weighted spatial-interaction models are the standard instrument for inferring plausible flows from observable attributes when full traceability is unavailable (Ferrari et al., 2022; Boonman et al., 2025; Siegrist et al., 2022). Models 1 and 2 are retained as an envelope of structural sensitivity. Because the model is parameterised on public attributes and not validated against observed flows, it is presented throughout as a reference specification rather than a representation of actual paddy movements.

3.6. Calibration of the Local-Processing Fraction and the Husk Ratio

Two fractions are used and must not be conflated: λ_res, the fraction applied to the residual competitive pool (after the exogenous deduction), which is the calibrated parameter; and λ_eff, the effective departmental fraction — paddy assigned to all modeled nodes divided by total departmental production — which is a reported outcome.

The local-processing fraction is calibrated against the Molino Barichara weighbridge series. Reconstructed annual throughputs are 25,461 t (2020), 28,060 t (2021) and 21,299 t (2022), corresponding to departmental shares of 2.573%, 2.435% and 1.930% (mean 2.312%). The calibration target is constructed as a share applied to the model's own production base, not as an absolute tonnage projected forward:

$$T_cal = mean\ share_{2020–2022} \times P^{cNA2023}_dept = 0.02312 \times 1{,}086{,}152 \approx 25{,}115\ t \quad (9)$$

Using the mean observed share rather than the mean observed tonnage removes the need to project absolute throughput to the base year and guarantees that the target is expressed on the same production base as the model. The calibrated value follows by dividing the target by the share the reference specification assigns to Barichara at full local processing, giving λ_res = 0.329.

The relationship between the model and the Barichara anchor is an identity, not an independent validation: The model reproduces at Barichara the value with which it was calibrated. No independent validation against observed flows is possible with public data, a limitation whose regulatory origin is documented in Section 3.9. Because a single anchor provides one equation and cannot simultaneously identify α, β and λ, the friction and attractiveness exponents are imposed as structural specifications (α = 1.5, β = 1) rather than estimated. Two structurally different uncertainty sources are propagated and reported separately rather than merged: A spatial band from a grid over α and β (sensitivity to model specification) and an interannual band from the 2020-2022 volatility of the anchor (sensitivity to temporal stability). Combining them would imply they are draws from a common distribution, which they are not.

3.6.1. Husk-to-paddy ratio

HPRdp is set at 0.22 on a dry-paddy basis, supported by three sources of different status: The Atlas del potencial energético de la biomasa residual en Colombia reports a rice-husk residue factor of 0.20 attributed to Fedearroz (UPME et al., 2010, Annex E, Table 29, p. 163), retained as the lower reference of the sensitivity range; UPRA (2020, Table 26, p. 111) reports 0.22 on an explicitly declared dry-paddy basis within a more recent sectoral instrument, adopted as the central value; and the Barichara weighbridge records an observed husk fraction of 22.1%, independently consistent with the UPRA figure. The adoption of 0.22 rather than 0.20 is therefore a traceable revision of a documented antecedent (S4). The sensitivity range is 0.18-0.25.

3.7. Rice Husk Generation, Availability and Energy Conversion

The green paddy allocated to each node is converted to dry paddy, then to generated husk, then to the energy-available fraction, and finally to a dry-husk equivalent. Because κg-d is constant, allocating green paddy before conversion is numerically equivalent to converting before allocating; the ordering is stated to match Figure 1:

$$Q^{dry}_\{j,t\} = Q^{green}_\{j,t\} \times \kappa_\{g\text{-}d\} \quad (10)$$

$$RH^{gen}_\{j,t\} = Q^{dry}_\{j,t\} \times HPR_\{dp\} \quad (11)$$

$$RH^{avail}_\{j,t\} = RH^{gen}_\{j,t\} \times A_f \quad (12)$$

$$RH^{dry}_\{j,t\} = RH^{avail}_\{j,t\} \times (1 - MC) \quad (13)$$

HPRdp yields generated husk prior to explicit moisture correction; the dry equivalent follows from the MC term in Equation (13), so moisture is subtracted exactly once. Moisture content is set at 0.08, 0.10 (central) and 0.15 on a wet basis, spanning the source literature (Mansaray and Ghaly, 1997; Olupot et al., 2016; Kamruzzaman et al., 2024; Wu et al., 2009). The availability factor *Af* takes values 0.25, 0.50, 0.75 and 1.00, with 0.50 central. It is a declared scenario variable rather than an observed rate: Husk in Casanare is committed in part to internal drying fuel, soil amendment and documented non-energy markets (Section 2.5) whose sector-wide volumes are not publicly recorded, so the four-point range brackets a resource governed by an undocumented but active set of competing uses.

Primary energy follows from dry husk mass and lower heating value; technical electricity follows from electrical conversion efficiency, with MJ converted to MWh by dividing by 3600:

$$E^{primary}_\{j,t\} = RH^{dry}_\{j,t\} \times 1000 \times LHV_dry \quad (14)$$

$$E^{electric}_\{j,t\} = (E^{primary}_\{j,t\} \times \eta_e)/3600\ [MWh/year,\ gross] \quad (15)$$

The factor 1000 converts tonnes to kilograms. LHV bounds (13.2 and 16.2 MJ/kg) derive from the dry-basis range of Mansaray and Ghaly (1997); the central value (14.1 MJ/kg) aligns with Wu et al. (2009) for an operational gasification plant. The conversion stage adopts rice husk biomass gasification coupled to an internal combustion engine-generator (BGPG) as the reference pathway: Husk is a point-source residue at mills, its moisture lies within the range suitable for gasification, and medium-scale BGPG is widely reported for decentralized applications (Natarajan et al., 1998; Olupot et al., 2016; Lenis Rodas et al., 2022). Combustion-steam cogeneration (Mujeebu et al., 2011) is not adopted, since mill-level steam demand is not modelled. Efficiency η_e is a technology-specific scenario parameter, not an observed value: 0.20 central and 0.25 high-performance (Wu et al., 2009). Equation (15) yields gross potential; where a net figure is reported, an auxiliary factor δaux = 0.15 is applied (Olupot et al., 2016). Bounding efficiencies (0.10, 0.30) appear as context in Table 5.

3.8. Scenario Design, Robustness Specifications and Sensitivity Analysis

The assessment is organized as a multi-parameter scenario design rather than a single point estimate. The parameters varied are λ, HPRdp, *Af*, MC, LHVdry and η_e (Table 5). Because the mass-energy chain is multiplicative, HPRdp, *Af*, LHVdry and η_e scale output proportionally when other parameters are held fixed, moisture enters through (1 - MC), and λ_res affects total output jointly with the fixed exogenous contribution. Reported scenario spans therefore reflect the width of the adopted ranges rather than intrinsic parameter elasticity.

Four robustness specifications are defined and reported in Section 4; their construction is detailed in Supplementary Material S5. In brief: (1) a cross-source check compares municipal shares from CNA 2023 against EVA 2024; (2) a structural check runs Models 1 and 2 alongside the reference and compares allocation concentration through the Herfindahl-Hirschman Index; (3) an inventory-completeness (distance-only) specification lets all eleven commercial nodes compete solely by inverse distance ($A_j = 1$), fully recalibrated, to bound the effect of the Tier 5 node; and (4) a material-basis check converts the one Tier 2 capacity reported without an explicit basis to a paddy-equivalent basis, fully recalibrated under each alternative.

3.9. Institutional Traceability of Mill-Level Data

Storage capacity - the parameter governing the $Size_j$ component of Equation (2) and, through the saturation of Equation (3), the effective discriminator of the allocation model - is subject to a national monthly reporting obligation to the rice information system SIRIARROZ (MADR, 2025, as amended by MADR, 2026). No aggregated public dataset derived from that obligation was available at the documentary cut-off, so the evidence hierarchy of Table 2 had to be reconstructed from a regional survey, corporate reports, press sources and one primary weighbridge series. The same limitation is independently recorded by UPRA (2020), which reports that mill location and capacity could not be obtained despite formal requests. The consequences for the model are stated where they arise: The Tier 5 exclusion (Section 3.3) and the absence of any independent validation of the allocation (Section 3.6). The regulatory channels involved are distinguished in Supplementary Material S6, and the policy significance of this gap is discussed in Section 5.2.

4. RESULTS

This section reports the outcome of the four-level traceability chain defined in Section 3, moving from the verified municipal production base, through the public mill inventory and its spatial attractiveness scoring, to the calibrated allocation of paddy, the resulting husk generation and, finally, the gross technical electricity potential. Estimates are reported as scenario ranges wherever the underlying parameter is a policy or modeling choice rather than a measured quantity. Throughout, quantities derived from the spatial allocation are described as model-implied rather than observed and are conditional on the (modelled) inventory and calibration assumptions. Tables 6-9 document, respectively, the mill inventory and attractiveness scores (Table 6), the comparison of allocation models (Table 7), the distance-only robustness specification (Table 8), and the departmental processing-fraction scenarios (Table 9); the full husk-and-energy balance by mill is reported in Supplementary Table S7.

4.1. Municipal Production Base and Cross-Source Robustness

The municipal paddy base for Casanare was verified row by row against the primary census source. The thirteen rice-producing municipalities of the department jointly account for a green-paddy production of 1,086,152 t in the CNA 2023 reference year (DANE et al., 2024), with the five largest producers — Paz de Ariporo, San Luis de Palenque, Maní, Nunchía and Yopal — concentrating 63.2% of departmental output. This census figure is the base on which the entire mass-energy chain is computed.

A cross-source robustness check compared the relative municipal shares of CNA 2023 against those of the EVA 2024 dataset (UPRA, 2024). The two sources are strongly correlated in their municipal distribution (Pearson $r = 0.937$; Spearman $\rho = 0.945$), with a total variation distance of 7.4% and a maximum single-municipality divergence of 3.70 percentage points, occurring in Nunchía. The two datasets therefore agree closely on the ranking of producing municipalities but not exactly on their shares; the allocation results reported below use CNA 2023.

4.2. Public Mill Inventory, Data Completeness and Modelling Regimes

The inventory audit identified twelve operational rice-milling nodes in Casanare at the July 2026 documentary cut-off,

Table 6: Public mill inventory and attractiveness scores (ten competitive nodes)

Mill	Municipality	Storage (t)	Capacity basis	Size	A_j
ORF S.A. - Pore	Pore	100,000	Durán Hernández et al. (2021)	1.000	1.000
Agroindustrial Sonora	Aguazul	100,000	Durán Hernández et al. (2021)	1.000	1.000
ORF S.A. - Villanueva	Villanueva	100,000	Durán Hernández et al. (2021)	1.000	1.000
Diana Corporación	Yopal	80,000	Durán Hernández et al. (2021)	0.787	0.936
Granos y Cereales de Colombia	Yopal	80,000	Durán Hernández et al. (2021)	0.787	0.936
Arrocera La Esmeralda	Aguazul	65,000	Corporate report (Blanquita, 2024)	0.626	0.888
Unión de Arroceros	Nunchía	40,000	Regional press (2022)	0.360	0.808
Molinos El Yopal	Yopal	30,000	Corporate, dry-paddy basis	0.253	0.776
Arroz Barichara	Yopal	6,300	Primary weighbridge	0.000	0.700
Molino Casanare	Yopal	8,570	Imputed (size-class)	0.024	0.557

Capacities attributed to Durán Hernández et al. (2021) are 2018 regional-survey estimates applied uniformly to every node for which no plant-specific source was located. The La Esmeralda figure is reported by the company as "tonnes of rice" without an explicit material basis and is treated as a nominal storage proxy. Molino Casanare's capacity is imputed by size-class regression, and its Act score is set to 0.5

Table 7: Comparison of spatial allocation models (ten-node residual pool)

Model	HHI	Largest receiving node	Top share (%)
M1 Nearest-neighbor	0.258	Unión de Arroceros (Nunchía)	31.6
M2 Pure gravity	0.107	ORF Pore	17.0
M3 Attractiveness-weighted gravity (reference)	0.112	ORF Pore	19.4

Table 8: Distance-only robustness specification for the capacity-undocumented node

Model	Nodes	λ_res	Electricity (GWh/yr)
Central: Capacity-weighted gravity (reference)	10	0.329	24.3
Robustness: Distance-only gravity, full inventory	11	0.301	22.4

partitioned by the completeness of the parameters required for capacity-weighted allocation. Ten met the minimum requirements — active registration under CIIU 1051, a reproducible coordinate and a storage-capacity parameter — with five capacities taken from the regional survey of Durán Hernández et al. (2021), four from plant-specific corporate, press or weighbridge evidence, and one (Molino Casanare) imputed through the size-class procedure (Table 6). The Fedearroz plant at Pore, a grower-association service facility rather than a commercial buyer, is incorporated through the exogenous capacity regime of Section 4.3. The twelfth node, Molinos Agroindustrial del Casanare, is active and commercially registered but has no publicly documented capacity after two independent audit rounds covering sixteen source categories; it was therefore excluded from the reference specification and evaluated only in the distance-based robustness test of Section 4.6.

The attractiveness index was computed for the ten competitive mills following Section 3.4, with capacities spanning 6,300 t (Barichara, primary weighbridge) to 100,000 t. Because the Act, Ev and Acc components saturate at their maxima for all nodes but one — every mill lying within 250 m of the routed network — the index reduces in practice to $A_j \approx 0.70 + 0.30 \cdot Size_j$, making the specification a storage-informed gravity model rather than a fully discriminating multi-criteria index.

4.3. Calibration of the Model-Implied Local-Processing Share

The residual local-processing fraction λ_res — the fraction of the residual municipal pool that the model assigns to the modelled competitive nodes — was calibrated against primary weighbridge data from Molino Barichara for 2020-2022, reconstructed from individual weighing records rather than summary-sheet totals, which contained running-accumulator artifacts. The reconstructed annual throughput was 25,461 t (2020), 28,060 t (2021) and 21,299 t (2022), corresponding to departmental shares of 2.573%, 2.435% and 1.930% (mean 2.312%). Applying this mean share to the CNA 2023 base gives a temporally consistent calibration target of 25,115 t, implying a storage turnover of approximately 4 times per year for Barichara, physically coherent for a small mill.

Because a single mill provides only one observation, the friction and attractiveness exponents ($\alpha = 1.5$, $\beta = 1$) are imposed as structural specifications rather than statistically estimated. Dividing the observed throughput by the share the attractiveness-weighted model predicts for Barichara at full local processing yields a calibrated residual processing fraction $\lambda_res = 0.329$. The relationship between the model and the calibration anchor is an identity, not an independent validation. Two distinct uncertainty bands are propagated: The spatial grid over α and β bounds λ_res between 0.253 and 0.447, while the interannual volatility of the anchor bounds it between 0.274 and 0.366.

The Fedearroz plant at Pore is incorporated through an exogenous capacity regime. Its annual throughput is estimated by applying a 75% utilization factor to its publicly documented milling capacity of 2,240 t of dry paddy per month (26,880 t/year; Federación Nacional de Arroceros, 2015), equivalent to approximately 24,000 t of green paddy per year. This intake is deducted from each municipality's production — concentrated in Pore municipality, which supplies 97.7% of the exogenous intake — before the ten competitive mills allocate the residual, preventing double counting.

4.4. Central Mass-Energy Balance

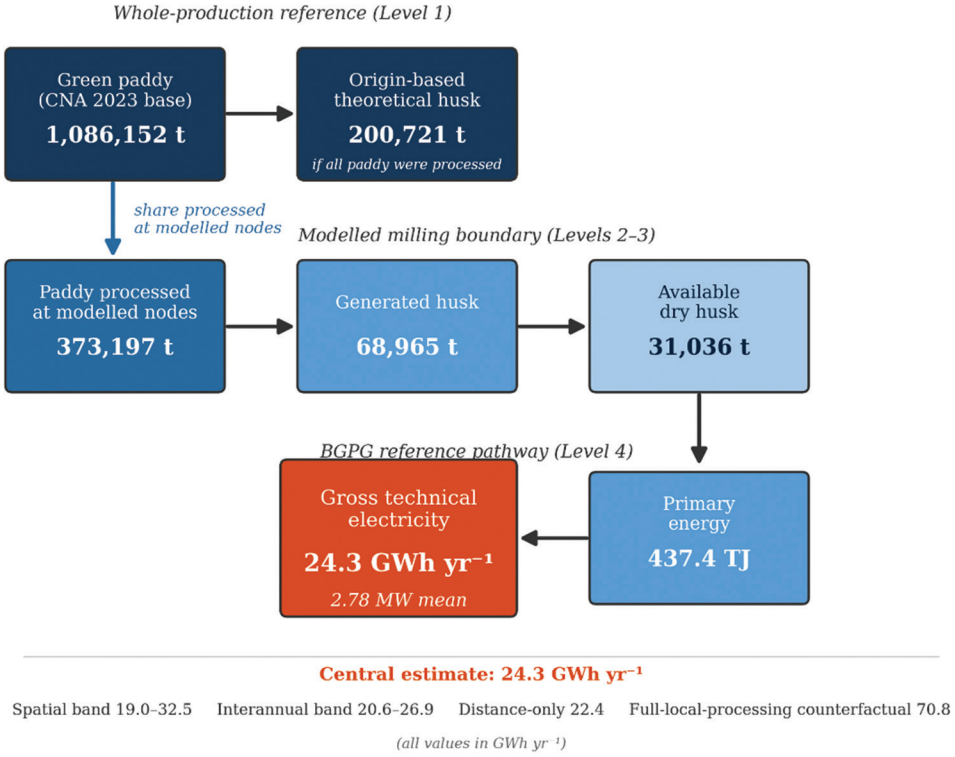
Applying the calibrated λ_res to the attractiveness-weighted allocation over the ten competitive nodes, and adding the exogenous Fedearroz node, produces the by-mill balance reported in Supplementary Table S7. Under the central parameter set ($HPR_dp = 0.22$, $A_f = 0.50$, $MC = 0.10$, $LHV_dry = 14.1$ MJ/kg, $\eta_e = 0.20$), the gross technical electricity potential from available rice husk in Casanare is 24.3 GWh/year, a mean continuous output of 2.78 MW, with an effective departmental processing fraction λ_eff of 0.344. Figure 3 traces the contraction from the CNA 2023 base through the modelled milling boundary to that result.

The CNA 2023 base of 1,086,152 t of green paddy implies 200,721 t of origin-based theoretical husk if all paddy were processed (whole-production reference, Level 1). The modelled milling boundary retains 373,197 t of processed paddy and yields 68,965 t of generated husk; availability and moisture adjustments reduce this to 31,036 t of available dry husk; and the reference BGPG pathway converts 437.4 TJ of primary energy into 24.3 GWh yr^{-1} of gross electricity. The spatial band is 19.0-32.5 GWh yr^{-1}, the interannual band 20.6-26.9 GWh yr^{-1}, the distance-only specification 22.4 GWh yr^{-1}, and the full-local-processing counterfactual 70.8 GWh yr^{-1}.

4.5. Spatial Separation between Paddy Origins and Mill-Located Potential

The spatial contribution of the assessment lies not in remapping municipal paddy production, which official agricultural sources already report, but in relocating the residue from agricultural origins to the milling nodes at which rice husk is modelled to become physically concentrated. Seven municipalities that jointly account for 66.8% of the CNA 2023 paddy total - Paz de Ariporo,

Figure 3: Contraction from origin-based rice-husk potential to gross technical electricity potential in Casanare



San Luis de Palenque, Maní, Trinidad, Tauramena, Orocué and Hato Corozal - contain no model-included milling node, whereas the ten competitive nodes and the Fedearroz node are concentrated in a five-municipality corridor comprising Yopal, Aguazul, Pore, Nunchía and Villanueva. The absence of verified milling nodes in the principal producing municipalities is an inventory-based finding; the resulting degree of concentration among receiving mills is conditional on the selected allocation specification. This separation is mapped in Figure 2, which also reports the resulting gross technical electricity potential by node; the municipal production surface represents agricultural origin only and should not be interpreted as the location of rice-husk generation or as a municipal electricity-potential map.

The inset resolves the overlapping Yopal-Aguazul nodes. (b) Gross technical electricity potential by node under the central scenario; the ten competitive nodes are allocated through the attractiveness-weighted gravity regime, whereas M-FED is incorporated through the exogenous capacity regime. Bars sum to 24.3 GWh yr^{-1}. The capacity-undocumented node evaluated only in the distance-only robustness specification is not assigned a central-scenario value.

4.6. Comparison of Allocation Models and Inventory-Completeness Robustness

The three allocation specifications defined in Section 3.5 were run over the ten-node residual pool. Table 7 reports their concentration (HHI) and largest receiving node. The nearest-neighbor model (Model 1) produces the most concentrated allocation (HHI 0.258); pure gravity (Model 2) and attractiveness-weighted gravity (Model 3) both spread paddy across more destinations (HHI 0.107 and 0.112), with the largest share at ORF Pore in both cases. Model 3 is retained as the reference specification.

To bound the effect of the one node without a documented capacity (Molinos Agroindustrial del Casanare), a distance-only robustness specification was run in which every commercial mill — the ten capacity-weighted nodes plus Molinos Agroindustrial — competes solely by inverse road distance ($A_j = 1$ for all eleven nodes), so that no capacity value is required for the excluded node. Under this specification the departmental technical potential is 22.4 GWh/year. Because this comparison changes the allocation rule for all eleven nodes rather than isolating Molinos Agroindustrial, it is a joint robustness check on modeling philosophy and inventory completeness; the combined alternative changes the departmental estimate by −7.8% relative to the reference specification.

4.7. Counterfactual, Scenario Span and Attractiveness Robustness

Table 9 reports the departmental technical potential across processing-fraction scenarios. Assigning the entire departmental production to Casanare nodes ($\lambda_{res} = 1$) under central availability and conversion parameters yields 70.8 GWh/year — a counterfactual under central parameters, not an absolute physical ceiling. The central estimate of 24.3 GWh/year therefore differs by 46.4 GWh/year (65.6%), reflecting the share of departmental paddy the model assigns to processing outside the included nodes: A modelled inference conditional on the inventory rather than an observed flow.

Because the mass-energy chain is multiplicative, HPR_{dp}, A_f, LHV_{dry} and η_e scale output proportionally when other parameters are held fixed; moisture enters through (1-MC), and λ_{res} affects total output jointly with the fixed Fedearroz contribution. The widest output span is associated with A_f (a

Table 9: Departmental technical electricity potential under processing-fraction scenarios

Scenario	λ_res	Electricity (GWh/year)	Difference versus full processing (GWh/year)
Lower bound (spatial grid)	0.253	19.0	51.7
Interannual low (2022)	0.274	20.6	50.2
Central (calibrated)	0.329	24.3	46.4
Interannual high (2020)	0.366	26.9	43.9
Upper bound (spatial grid)	0.447	32.5	38.2
Full local processing	1.000	70.8	0.0

factor of 4.0 across 0.25-1.00), followed by the processing-fraction scenarios and HPR_dp, with conversion parameters producing narrower spans — an ordering that reflects the width of the adopted ranges rather than intrinsic elasticity. The specific electricity yield is 783 kWh per tonne of dry husk at central parameters, ranging from approximately 733 to 1,125 kWh across the LHV range (13.2-16.2 MJ/kg) and the executed efficiency scenarios (η_e = 0.20-0.25).

A final robustness test addresses the one capacity figure reported without an explicit material basis: Treating the Arrocera La Esmeralda value as milled white rice and converting it to a paddy-equivalent basis (93,000-100,000 t), with full recalibration under each alternative, changes the departmental total by approximately 1-1.5%. The central result is therefore robust to the unresolved material basis of this single figure.

5. DISCUSSION

The results show why a departmental biomass assessment should not be expressed as a single residue total. The four-level chain converts an agricultural production base into progressively more restrictive quantities, and each reduction has a different interpretation for energy planning. The central estimate is therefore not simply a smaller version of the theoretical potential: It is the outcome of a sequence of spatial, operational, and technological conditions that determine where rice husk is generated, how much may remain available, and how much gross electricity could be produced under the reference pathway.

5.1. Interpreting the Estimate

The four-level chain matters because each level answers a different question and collapsing them produces a category error. The contraction shown in Figure 3 is driven mainly by the estimated location of processing rather than by any physical loss of biomass: Paddy assigned to mills outside the modelled network still generates husk, but not at facilities available for regional energy planning. Agricultural origin and agro-industrial residue location are therefore related but not interchangeable, which is the central contribution of the allocation stage. The availability and moisture adjustments represent distinct mechanisms — competing uses on one hand, mass-basis conversion on the other — and conflating them would misstate the resource in opposite directions. The fourth level yields a comparable technical potential under a defined gasification pathway, not a plant design or a forecast of delivered electricity.

Uncertainty is unevenly distributed and of two kinds. The availability factor produces the widest output span, but this reflects the width of the adopted interval rather than intrinsic elasticity; the central value is an operational regime representing partial internal or competing use, not an observed rate. The structurally decisive parameter is the local-processing fraction, because it determines how much of the departmental base enters the modelled network. Unlike the material properties, it is not a physical constant: It summarises unobserved commercial flows, cross-departmental processing and inventory coverage, and calibration against one mill makes the central scenario locally grounded without converting it into an observed departmental share. The results are broadly consistent with the residual-biomass literature, which documents the same declining sequence when gross generation is progressively adjusted for competing uses (Chauhan, 2010; Kongchouy et al., 2021), and with mill-scale rice-husk assessments reporting comparable orders of magnitude and decentralised processing configurations (Kapur et al., 1996; Ejiofor et al., 2020; Thengane et al., 2020; Lenis Rodas et al., 2022). A detailed level-by-level interpretation, the full scenario analysis and an extended comparison with previous studies are provided in Supplementary Material S8.

5.2. Territorial and Policy Implications

The spatial results reveal a marked separation between agricultural origins and milling destinations (Figure 2): Seven municipalities accounting for approximately two thirds of departmental paddy contain no verified milling node, whereas the modelled facilities concentrate in the Yopal-Aguazul-Pore-Nunchía-Villanueva corridor. For territorial planning, maps of crop production alone would misrepresent the locations at which husk becomes physically concentrated and manageable as an energy feedstock.

The comparison among allocation models shows why nearest-neighbour assignment is insufficient as a reference representation of commercial processing: It concentrates 31.6% of the residual flow at one node (HHI 0.258), whereas the gravity specifications distribute flows more broadly (HHI 0.107-0.112). This is consistent with Bojesen et al. (2014), who treated biomass destinations as competing alternatives, and with Karg et al. (2025), whose food-flow evidence shows that distance matters together with destination scale and access. The dual-regime structure is likewise empirically motivated: When the Fedearroz service plant was provisionally allowed to compete on attractiveness, the model assigned it approximately 2.1 times its declared physical capacity, confirming that a grower-association plant serving a defined membership does not behave like a commercial buyer.

The allocation should nevertheless not be read as an observed procurement network. Because most non-size components of the index reach their maxima, the reference model operates largely as a storage-informed gravity specification: Useful for identifying plausible concentration patterns, but unable to reveal contracts, prices, ownership links or actual cross-border flows. The appropriate policy use is screening — identifying priority mill corridors for data collection, energy-demand matching and subsequent feasibility assessment.

These screening results connect directly to Colombian energy-planning instruments. The National Energy Plan proposes a network of regional Bio-Hubs to promote the energy use of residual biomass and states the intention of integrating them into the National Interconnected System under distributed-generation or self-generation arrangements (UPME, 2025a); at the departmental level, science and technology planning explicitly prioritises rice-husk valorisation for energy (Gob Casanare, 2015). A concentration of husk generation in an identifiable milling corridor is precisely the spatial precondition such a hub-based policy requires. The national coverage-expansion instrument, for its part, does not yet develop a specific pathway for residual biomass (UPME, 2025b), so the resource remains more clearly articulated in strategic planning than in the instruments that programme rural electrification investment.

Moving this assessment from inference toward measurement depends on data already collected by the State. Mills and agro-industrial actors must report volumes traded and storage capacity monthly to the rice information system SIRIARROZ under a monitored-freedom price regime (MADR, 2025, as amended by MADR, 2026) — storage capacity being the very parameter that governs the allocation model and whose absence forced one node out of the reference specification. This obligation is recent, established in 2025, so aggregated series may become available in the near term and would offer a level of external validation not currently possible. A comparable pattern appears in industrial statistics, where the Annual Manufacturing Survey records husk consumption and its allocation to self-generation and cogeneration (DANE, 2024), and in sector planning, where UPRA reports that mill location and capacity could not be obtained despite formal requests (UPRA, 2020). The policy implication is narrow and actionable: Publishing already-collected mill-level throughput and husk-use data would allow the allocation and availability stages to move from scenario-based inference toward empirical calibration, without imposing any new reporting burden. The results support screening and prioritisation of milling corridors for such data collection; they do not identify a plant site, recommend an investment, or establish a proven supply option for remaining isolated localities.

5.3. Uncertainty, Robustness and Scope

Several results increase confidence in the framework without constituting validation. Municipal production shares are stable across two official sources, the alternative material basis for the one ambiguous capacity figure changes the departmental total by only 1-1.5%, and the distance-only full-inventory specification changes the central estimate by −7.8%. The total is therefore not dominated by a single disputed capacity value or inventory exclusion.

The strongest uncertainties remain structural, and they define the proper interpretation of the study. The processing share is calibrated from one mill; the distance and attractiveness exponents are imposed rather than estimated; several storage capacities are historical proxies rather than current throughput, and storage capacity does not measure annual milling capacity directly; the Fedearroz contribution depends on an assumed utilisation rate; and the availability factor is uniform across mills even though internal heat demand, sales and residue-management practices are likely heterogeneous. Annual totals also suppress the pronounced seasonal concentration of the Casanare harvest, and gross electricity excludes auxiliary consumption without establishing net delivery, dispatchability or coincidence with local demand. The framework consequently narrows a theoretical agricultural resource into a transparent, model-implied technical potential and identifies where better information would most improve the estimate; it does not establish economic viability, environmental superiority or an implementable plant portfolio. Until municipality-to-mill purchase data, current plant throughput and mill-specific husk-use balances become available, the value of the results is comparative and planning-oriented.

6. CONCLUSION

This study estimated the rice-husk electricity potential of Casanare through a spatially explicit, four-level traceability chain that separates agricultural production, agro-industrial residue generation, availability under competing uses, and technical electricity potential. Applied to a verified base of 1,086,152 t of green paddy across thirteen municipalities and calibrated against primary weighbridge data, the framework yields a central estimate of 24.3 GWh/year of gross technical electricity — a mean continuous output of 2.78 MW — under the reference gasification pathway. Structural uncertainty is reported as two separate bands: A spatial band of 19.0-32.5 GWh/year from the imposed allocation exponents, and an interannual band of 20.6-26.9 GWh/year from the temporal stability of the calibration anchor. A full-local-processing counterfactual of 70.8 GWh/year shows that the boundary of the included milling nodes, not the conversion technology, is the principal determinant of the estimate.

Three findings carry beyond the specific figures. First, agricultural origin and agro-industrial residue location are not interchangeable: Seven municipalities that jointly originate roughly two-thirds of departmental paddy contain no operational milling node, while generation concentrates in a five-municipality corridor. A resource map built from crop production alone would misplace the point at which husk becomes physically manageable as a feedstock. Second, the estimate is governed less by the energy parameters than by two structural quantities that public data do not observe: The share of paddy processed within the modelled inventory, and the fraction of husk left uncommitted after competing uses. Third, the recent integration of formerly non-interconnected rice-producing municipalities into the national grid reframes this husk as a candidate contributor to interconnected supply in a department that retains a pronounced rural access gap.

The principal contribution is methodological and replicable: A defensible municipality-to-mill allocation can be constructed entirely from public registry, road-network and capacity evidence, provided an explicit evidence hierarchy governs which facilities enter the model. The same exercise exposes a data gap of direct policy relevance - mill throughput, storage capacity and husk-use allocation are already collected under existing reporting or statistical obligations in Colombia, yet none is published as a public aggregate. Publishing already-collected data, rather than

imposing new reporting, is the single change that would most improve assessments of this kind.

Within the limitations set out in Section 5.3, the estimate should be read as a comparable technical potential for territorial planning rather than a statement of economic viability or an implementable plant portfolio. Future work should incorporate the intra-annual concentration of supply, which determines whether continuous generation is feasible without storage; extend the allocation to remaining isolated localities through an explicit husk-transport assessment; and replace the modelled allocation with observed municipality-to-mill flows should the underlying data become available. A subsequent techno-economic stage could then estimate the levelised cost of husk-based gasification and assess whether it can compete within the existing generation mix of the region.

7. ACKNOWLEDGMENTS

The authors thank Molino Barichara for providing the weighbridge records used to calibrate the allocation model.

8. DISCLOSURE OF AI USE

Artificial-intelligence language models (OpenAI GPT-5.x; Anthropic Claude Opus 4.x) were used to assist with documentary source verification. All methodological decisions, calculations, results and their interpretation are the authors' own, and the authors reviewed and verified all AI-assisted text.

REFERENCES

Barrera Hernández, J.C., Sagastume Gutiérrez, A., Ramírez-Contreras, N.E., Cabello Eras, J.J., García-Núñez, J.A., Barrera Agudelo, O.R., Silva Lora, E.E. (2024), Biomass-based energy potential from the oil palm agroindustry in Colombia: A path to low carbon energy transition. Journal of Cleaner Production, 449, 141808.

Bojesen, M., Birkin, M., Clarke, G. (2014), Spatial competition for biogas production using insights from retail location models. Energy, 68, 617-628.

Boonman, A., Fukuda, S., Tiwari, S., Kraxner, F. (2025), Two-phase approach for designing sustainable biomass supply chains for community-scale biomass power plants in Thailand. Energies, 18(3), 520.

Bressanin, J.M., Guimarães, H.R., Chagas, M.F., Sampaio, I.L.M., Klein, B.C., Watanabe, M.D.B., Bonomi, A., Morais, E.R., Cavalett, O. (2021), Advanced technologies for electricity production in the sugarcane value chain are a strategic option in a carbon reward policy context. Energy Policy, 159, 112637.

Chauhan, S. (2010), Biomass resources assessment for power generation: A case study from Haryana State, India. Biomass and Bioenergy, 34(9), 1300-1308.

Colciencias, Gobernación de Casanare, Observatorio Colombiano de Ciencia y Tecnología. (2012), Plan Estratégico Departamental de Ciencia, Tecnología e Innovación de Casanare (PEDCTI). Bogotá: Colciencias. Available from: https://minciencias.gov.co/sites/default/files/upload/paginas/pedcti-casanare.pdf

DANE, Fedearroz, FNA. (2024), Quinto Censo Nacional Arrocero (5 CNA) 2023: Zona Llanos. Bogotá: Departamento Administrativo Nacional de Estadística. Available from: https://www.dane.gov.co/files/operaciones/cna/bol-5tocna-2023.pdf

DANE, Fedearroz, FNA. (2026), Encuesta Nacional de Arroz Mecanizado (ENAM): Segundo Semestre 2025. Bogotá: Departamento Administrativo Nacional de Estadística. Available from: https://www.dane.gov.co/files/operaciones/enam/bol-enam-iisem2025.pdf

DANE. (2014), Cuenta Satélite Piloto de la Agroindustria del Arroz 2005-2012. Bogotá: Departamento Administrativo Nacional de Estadística. Available from: https://www.dane.gov.co/files/investigaciones/pib/agroindustria/guia_pro_resulcspa_arroz2005_2012.pdf

DANE. (2024), Encuesta Anual Manufacturera (EAM): Diccionario de Variables. Bogotá: Departamento Administrativo Nacional de Estadística. Available from: https://www.dane.gov.co/index.php/estadisticas/por/tema/industria/encuesta/anual/manufacturera-enam

De Souza, N.R.D., Duft, D.G., Bruno, K.M.B., Henzler, D.S., Junqueira, T.L., Cavalett, O., Hernandes, T.A.D. (2021), Unraveling the potential of sugarcane electricity for climate change mitigation in Brazil. Resources, Conservation and Recycling, 175, 105878.

Durán Hernández, Z.L., Barrera Amaya, J.O., Ardila Cuevas, J.A. (2021), Cultivo del arroz en la cuenca media y baja del río Cravo sur. In: Antelo Albertos, R., Díaz Olaya, M., Del R., Durán Hernández, Z.L., Rojano, C., editors. El Reto de Conservar y Producir. Sello Editorial UNAD, pp. 350-383.

Ejiofor, O.S., Okoro, P.A., Ogbuefi, U.C., Nnabuike, C.V., Okedu, K.E. (2020), Off-grid electricity generation in Nigeria based on rice husk gasification technology. Cleaner Engineering and Technology, 1, 100009.

Federación Nacional de Arroceros. (2015), Fedearroz Inaugura Primera Planta de Secamiento, Almacenamiento y Trilla. Available from: https://www.fedearroz.com.co/es/noticias/2015/08/26/fedearroz-inaugura-primera-planta-de-secamiento-almacenamiento-y-trilla

Federación Nacional de Arroceros. (n.d.), Planta de Pore. Available from: https://www.fedearroz.com.co/es/la-federacion/donde-estamos/plantas/planta-de-pore [Last accessed on 2026 Jul 15].

Ferrari, G., Marinello, F., Lemmer, A., Ranzato, C., Pezzuolo, A. (2022), Network analysis for optimal biomethane plant location through a multidisciplinary approach. Journal of Cleaner Production, 378, 134484.

Fioranelli, A., Bizzo, W.A. (2023), Generation of surplus electricity in sugarcane mills from sugarcane bagasse and straw: Challenges, failures and opportunities. Renewable and Sustainable Energy Reviews, 186, 113647.

Furtado, L.A., Ribeiro, S.G., Pradelle, F., Parise, J.A.R. (2023), Modeling and techno-economic analysis of a hybrid sugarcane plant fed by vinasse biogas and bagasse surplus for electricity generation. Journal of Cleaner Production, 413, 137511.

Gobernación de Casanare, Colciencias. (2015), Plan y Acuerdo Estratégico Departamental de Ciencia, Tecnología e Innovación de Casanare (PAED). Bogotá: Ministerio de Ciencia, Tecnología e Innovación. Available from: https://minciencias.gov.co/sites/default/files/upload/paginas/paed-casanare.pdf

Grupo Empresarial Blanquita. (2024), Informe de Sostenibilidad 2022-2023. Available from: https://www.blanquita.com.co/blanquita/wp-content/uploads/2024/05/informe-2023-2022-sostenibilidad-blanquita.pdf

ICA. (2020), Resolución No. 780006 de 2020: Requisitos Para el Registro de Viveros y la Producción de Material de Propagación. Bogotá: Instituto Colombiano Agropecuario.

ICA. (2022), Resolución No. 00004706 de 2022: Requisitos Para el Registro Ante el ICA de Los Lugares de Producción de Arroz Paddy. Bogotá: Instituto Colombiano Agropecuario. Available from: https://www.ica.gov.co/getattachment/65f8b861-9a2f-448d-9edf-6813b6e9afe9/2022r0004706.aspx

IPSE. (2023), Las Localidades de Bocas de Pauto (Casanare) y Santa Rosalía (Vichada) Entraron a Finales de Febrero 2023 al Sistema Interconectado Nacional. Bogotá: Instituto de Planificación

y Promoción de Soluciones Energéticas para las Zonas No Interconectadas. Available from: https://ipse.gov.co/blog/2023/03/28

Jain, S. (2026), Mapping global cereal flows at subnational scales uncovers heterogeneities in sourcing dependencies. Environmental Research: Food Systems, 3(2), 021002.

Jyothsna, G., Bahurudeen, A., Sahu, P.K. (2024), Sustainable utilisation of rice husk for cleaner energy: A circular economy between agricultural, energy and construction sectors. Materials Today Sustainability, 25, 100667.

Kamruzzaman, M., Shahriyar, M., Bhuiyan, A.A., Bhattacharjya, D.K., Islam, M.K., Alam, E. (2024), Energy potential of biomass from rice husks in Bangladesh: An experimental study for thermochemical and physical characterization. Energy Reports, 11, 3450-3460.

Kapur, T., Kandpal, T.C., Garg, H.P. (1996), Electricity generation from rice husk in Indian rice mills: Potential and financial viability. Biomass and Bioenergy, 10(5-6), 393-403.

Karg, H., Bellwood-Howard, I., Ramankutty, N. (2025), How cities source their food: Spatial interactions in West African urban food supply. Food Security, 17(2), 439-460.

Kongchouy, P., Tia, W., Nathakaranakule, A., Soponronnarit, S. (2021), Assessment of seasonal availability and spatial distribution of bio-feedstock for power generation in Thailand. Bioenergy Research, 14(1), 70-90.

Laasasenaho, K., Lensu, A., Lauhanen, R., Rintala, J. (2019), GIS-data related route optimization, hierarchical clustering, location optimization, and kernel density methods are useful for promoting distributed bioenergy plant planning in rural areas. Sustainable Energy Technologies and Assessments, 32, 47-57.

Lenis Rodas, Y.A., Morales Rojas, A.D., Jaramillo Marín, S., Salcedo Jiménez, C., Pérez Bayer, J.F. (2022), Rice husk fixed bed gasification for circular economy in compact rice mills. Energy Sources Part a Recovery Utilization and Environmental Effects, 44(1), 1875-1887.

Luxen, D., Vetter, C. (2011), Real-Time Routing with OpenStreetMap data. In: Proceedings of the 19th ACM SIGSPATIAL International Conference on Advances in Geographic Information Systems. ACM. p513-516.

MADR. (2025), Resolución No. 000085 de 2025: Régimen de Libertad Vigilada del Precio del Arroz Paddy Verde, Arroz Paddy Seco, Arroz Blanco y sus Subproductos. Bogotá: Ministerio de Agricultura y Desarrollo Rural. Available from: https://www.suin-juriscol.gov.co/viewdocument.asp?id=30054823

MADR. (2026), Resolución No. 000047 de 2026: Modifica la Resolución No. 000085 de 2025. Bogotá: Ministerio de Agricultura y Desarrollo Rural. Available from: https://www.imex.com.co/sites/default/files/documentos/imex/news/26.%20minagricultura%20-%20resoluci%c3%b3n%20no.%2047%20del%2019.02.2026.pdf

Mansaray, K.G., Ghaly, A.E. (1997), Physical and thermochemical properties of rice husk. Energy Sources, 19(9), 989-1004.

Medina Medina, M.M., Sierra Carrillo, S.J. (2022), Determinación del Potencial de Biomasa Para Suministro de Energía Eléctrica en el Departamento del Casanare [Undergraduate Thesis]. Bucaramanga: Universidad Autónoma de Bucaramanga. Available from: http://hdl.handle.net/20.500.12749/18766

Molinos El Yopal, S.A.S. (n.d.), Conoce a Molinos El Yopal, la Empresa Detrás de Arroz Casanare. Available from: https://arrozcasanare.com/conocenos [Last accessed on 2026 Jul 15].

Monsalve Camacho, O.I., Henao Toro, M.C., Gutiérrez Díaz, J.S. (2021), Caracterización de materiales con uso potencial como sustratos en sistemas de cultivo sin suelo. Ciencia y Tecnología Agropecuaria, 22(1), e1977.

Montoya, J., Valdés, C., Chaquea, H., Pecha, M.B., Chejne, F. (2020), Surplus electricity production and LCOE estimation in Colombian palm oil mills using empty fresh bunches (EFB) as fuel. Energy, 202, 117713.

Mujeebu, M.A., Abdullah, M.Z., Ashok, S. (2011), Husk-fueled steam turbine cogeneration for a rice mill with power export: A case study. Energy Sources, Part A: Recovery, Utilization, and Environmental Effects, 33(8), 724-734.

Natarajan, E., Nordin, A., Rao, A.N. (1998), Overview of combustion and gasification of rice husk in fluidized bed reactors. Biomass and Bioenergy, 14(5-6), 533-546.

Olupot, P.W., Candia, A., Menya, E., Walozi, R. (2016), Characterization of rice husk varieties in Uganda for biofuels and their techno-economic feasibility in gasification. Chemical Engineering Research and Design, 107, 63-72.

OpenStreetMap contributors. (2026), OpenStreetMap [Data Set]. OpenStreetMap Foundation. Available from: https://www.openstreetmap.org

Pérez-Rodríguez, C.P., Ríos, L.A., Duarte González, C.S., Montaña, A., García-Marroquín, C. (2022), Harnessing residual biomass as a renewable energy source in Colombia: A potential gasification scenario. Sustainability, 14(19), 12537.

Prensa Libre Casanare. (2022), Arroz Supremo Absorberá el 15% de la Cosecha Arrocera del Casanare con su Nuevo Molino en Nunchía. Available from: https://prensalibrecasanare.com/casanare/45661

Ramírez Contreras, N.E., Arévalo, A., García-Núñez, J.A. (2015), Inventario de la biomasa disponible en plantas de beneficio para su aprovechamiento y caracterización fisicoquímica. Revista Palmas, 36(4), 41-54.

RUES. (2026), Consulta de Matrículas Mercantiles - Cámara de Comercio de Casanare [Data Set]. Confecámaras. Available from: https://www.rues.org.co

Sagastume Gutiérrez, A., Cabello Eras, J.J., Hens, L., Vandecasteele, C. (2020), The energy potential of agriculture, agroindustrial, livestock, and slaughterhouse biomass wastes through direct combustion and anaerobic digestion: The case of Colombia. Journal of Cleaner Production, 269, 122317.

Schlaich, T., Horn, A.L., Fuhrmann, M., Friedrich, H. (2020), A gravity-based food flow model to identify the source of foodborne disease outbreaks. International Journal of Environmental Research and Public Health, 17(2), 444.

Siegrist, A., Bowman, G., Burg, V. (2022), Energy generation potentials from agricultural residues: The influence of techno-spatial restrictions on biomethane, electricity, and heat production. Applied Energy, 327, 120075.

Singlitico, A., Kilgallon, I., Goggins, J., Monaghan, R.F.D. (2019), GIS-based techno-economic optimisation of a regional supply chain for large-scale deployment of bio-SNG in a natural gas network. Applied Energy, 250, 1036-1052.

Thengane, S.K., Burek, J., Kung, K.S., Ghoniem, A.F., Sanchez, D.L. (2020), Life cycle assessment of rice husk torrefaction and prospects for decentralized facilities at rice mills. Journal of Cleaner Production, 275, 123177.

UPME, IDEAM, Colciencias, Universidad Industrial de Santander. (2010), Atlas del Potencial Energético de la Biomasa Residual en Colombia. Bogotá: Unidad de Planeación Minero Energética. Available from: https://repositoriobi.minenergia.gov.co/handle/123456789/2413

UPME. (2025a), Plan Energético Nacional 2024-2054: Tomo I. Bogotá: Unidad de Planeación Minero Energética. Available from: https://docs.upme.gov.co/demandayeficiencia/documents/pen_2024_2054

UPME. (2025b), Plan Indicativo de Expansión de Cobertura de Energía Eléctrica (PIEC) 2024-2028. Bogotá: Unidad de Planeación Minero Energética. Available from: https://docs.upme.gov.co/simec/energia%20electrica/piec/2024-2028

UPME. (2025c), Índice de Cobertura de Energía Eléctrica (ICEE) 2024: Anexo Departamental y Municipal [Data Set]. Bogotá: Unidad de

Planeación Minero Energética. Available from: https://docs.upme.gov.co/simec/energia%20electrica/documents/informes_cobertura

UPRA. (2020), Plan de Ordenamiento Productivo del Sistema Arroz en Colombia 2020-2038. Bogotá: Unidad de Planificación Rural Agropecuaria, Ministerio de Agricultura y Desarrollo Rural.

UPRA. (2024), Evaluaciones Agropecuarias Municipales (EVA) 2024 - Casanare [Data Set]. Agronet/Ministerio de Agricultura y Desarrollo Rural. Available from: https://www.agronet.gov.co

Wu, C.Z., Yin, X.L., Ma, L.L., Zhou, Z.Q., Chen, H.P. (2009), Operational characteristics of a 1.2-MW biomass gasification and power generation plant. Biotechnology Advances, 27(5), 588-592.

XM S.A. E.S.P. (2023), 18 Proyectos Nuevos Ingresaron en el Primer Trimestre de 2023 al Sistema Interconectado Nacional. Available from: https://www.xm.com.co/noticias/5801

SUPPLEMENTARY MATERIAL

Rice husk power generation potential in Casanare, Colombia: a production-to-mill spatial assessment

This Supplementary Material documents the extended justifications, declared-but-unexecuted specifications, and robustness-construction details referenced from the main text (S1–S8). It is intended to be read alongside Sections 3 and 4 of the article.

S1. DECLARED DEPARTMENTAL-ANCHORING SPECIFICATION (NOT EXECUTED)

Referenced from Section 3.2. All results in the article are computed on the CNA 2023 municipal distribution. For years in which only a departmental total is published, the following share-preserving specification keeps the procedure updatable, where s □ {CNA2023, EVA2024} is the municipal specification and t_0 the last year with municipal data:

$$P^{adj_s}_\{i,2025\} = (P^s_\{i,t_0\} / \Sigma_i P^s_\{i,t_0\}) \times P^{ENAM}_\{Casanare,2025\} \quad (S1)$$

Equation (S1) rests on a spatial-stability assumption: that relative municipal shares are constant between t_0 and the anchoring year. It is declared for reproducibility and future updating only and is not applied to the reported results. Applying a 2025 departmental anchor (ENAM: 1,224,167 t) to a 2023 municipal distribution would introduce a temporal inconsistency between the production base and the 2020–2022 calibration anchor (Section 3.6), without improving the spatial resolution the allocation model requires. The ENAM departmental magnitude is used in the main text only as a scale reference.

S2. EVIDENCE-HIERARCHY PROPERTIES GOVERNING NODE INCLUSION

Referenced from Sections 3.3 and 3.4. Two properties of the capacity evidence hierarchy (Table II) govern the results.

Uniform application of Tier 3. Durán et al. (2021) is a single regional survey covering several plants. Once admitted as an acceptable capacity source for any node, consistency requires admitting it for every node lacking a higher-tier source; applying it selectively would make node inclusion depend on the order in which sources were retrieved rather than on the evidence available.

Absence of capacity treated as an information gap, not zero. For the single node reaching Tier 5 (Molinos Agroindustrial del Casanare), two independent audit rounds covering sixteen source categories — commercial registry, equipment suppliers, import records, environmental files searched by tax identification number, financial directories, corporate networks and direct contact — retrieved no storage, drying or milling-capacity figure. Because the capacity-weighted specification cannot represent a node without a capacity value, the node is excluded from the reference specification and its effect is bounded through the distance-only specification of S5, in which no capacity value is required. The node is therefore absent from the central model because of an evidentiary limit, not because it was assessed as inactive.

Concentration of empirical content. Because Act_j, Ev_j and Acc_j saturate at their maxima for all nodes but one, the attractiveness index reduces in practice to $A_j \approx 0.70 + 0.30 \cdot Size_j$ (Equation 3). The specification is thus more precisely a storage-informed gravity model than a fully discriminating multi-criteria index; the four-component structure is retained because it makes this saturation visible and because the non-saturating components would discriminate given richer registry data.

S3. DISTANCE-MATRIX VERIFICATION AND REJECTED CATEGORICAL SIZE RULE

Referenced from Section 3.4. As a backward-compatibility control, the expanded 13 × 10 origin–destination matrix was verified against the original eight-node matrix and reproduced it with a mean discrepancy of 16 m after two municipal coordinates (Monterrey and Nunchía) were identified as incorrectly reconstructed and corrected.

A discrete size-class rule for the $Size_j$ component was tested and rejected. Because the capacity distribution is heavily clustered at the upper end, discrete classes assigned nearly all nodes an identical score, which made Equation (2) collapse onto a near-constant and rendered the attractiveness-weighted model numerically indistinguishable from pure gravity. Continuous min–max normalization preserves the discrimination the index is intended to provide.

S4. HUSK-TO-PADDY RATIO: DUAL-ANCHOR DERIVATION

Referenced from Section 3.6. HPRdp = 0.22 (dry-paddy basis) is adopted as central, supported by three sources of different status:

Status	Source	Value	Basis
Regional antecedent (lower reference)	UPME et al. (2010), Annex E, Table 29, p. 163	0.20	residue-per-product; factor attributed to Fedearroz
Adopted central value	UPRA (2020), Table 26, p. 111	0.22	explicitly declared dry-paddy basis
Primary corroboration	Barichara weighbridge assay	0.221	11 milling-yield assays, study area

The adoption of 0.22 rather than 0.20 is a traceable revision of a documented antecedent: the earlier value derives from a national compilation whose rice coefficient is a federation-supplied figure, whereas the adopted value comes from a more recent instrument with an explicit basis and is corroborated by primary measurement in the study area. The sensitivity range (0.18–0.25) spans the antecedent value and the upper literature range.

S5. CONSTRUCTION OF THE FOUR ROBUSTNESS SPECIFICATIONS

Referenced from Section 3.8. Results are reported in Sections 4.1 and 4.6–4.7.

1. Cross-source robustness. Municipal shares from CNA 2023 are compared against EVA 2024 (Pearson and Spearman correlations, total variation distance, maximum single-municipality divergence) to establish whether the allocation depends on the choice of public municipal dataset.
2. Structural robustness of the allocation rule. Models 1 and 2 are run alongside the reference specification, with allocation concentration compared through the Herfindahl–Hirschman Index (HHI). The HHI is used as a model discriminator: it reports whether the specifications differ in the structure of the allocation and not merely in totals.
3. Inventory-completeness robustness (distance-only specification). All eleven commercial nodes — the ten capacity-weighted nodes plus the capacity-undocumented Tier 5 node — compete solely by inverse road distance, setting $A_j = 1$ for all nodes so that no capacity value is required, with the model fully recalibrated. Because this changes the allocation rule for all eleven nodes rather than isolating one, it is a joint robustness check on modeling philosophy and inventory completeness, not an isolated measurement of the missing node's contribution.
4. Material-basis robustness. Because one Tier 2 capacity figure (Arrocera La Esmeralda) is reported by the company without an explicit material basis, an alternative treatment converts it to a paddy-equivalent basis, with the model fully recalibrated under each alternative.

S6. REGULATORY CHANNELS OF THE RICE TRACEABILITY AND PRICE FRAMEWORK

Referenced from Section 3.9. The instruments relevant to mill-level flow information belong to distinct regulatory channels, which should not be conflated.

Channel	Instrument	Relevance to this study
Production-site traceability	ICA Resolution No. 00004706 of 2022 (ICA, 2022)	Institutional definition of a rice mill; registration of paddy production sites
Monitored-freedom price regime	MADR Resolution No. 000085 of 2025 (MADR, 2025a), as modified by MADR Resolution No. 000047 of 2026 (MADR, 2026b)	Article 3 and 5 reporting obligation (prices, volumes, inventories, storage capacity) to SIRIARROZ — the correct legal anchor for the reporting obligation
Regulated-price regime	MADR Resolution No. 000241 of 2025 (MADR, 2025b), replaced by MADR Resolution No. 000042 of 2026 (MADR, 2026a)	Distinct regulatory axis; includes SIRIARROZ price/purchase reporting but is not the general source of the reporting obligation
Sector-stabilization agreement	SIC Resolution No. 65722 of 2025 (SIC, 2025)	Authorized a sector-stabilization agreement; not the legal source of the reporting obligation

The variables mandated under Article 2 of Resolution 000085 of 2025 — volumes traded, and storage capacity in particular — correspond closely to the quantities this study reconstructed from fragmentary public evidence. A national reporting obligation covering these variables has been in force since 2025, yet no aggregated public dataset derived from it is available. This gap is independently corroborated by UPRA (2020), which records that mill location and capacity could not be obtained despite formal requests to the rice federation and the Ministry.

SUPPLEMENTARY REFERENCES

MADR. (2025b), Resolución No. 000241 de 2025: Régimen de libertad regulada de precios para arroz paddy verde. Bogotá: Ministerio de Agricultura y Desarrollo Rural.

MADR. (2026a), Resolución No. 000042 de 2026: Régimen de libertad regulada para arroz paddy verde y su equivalente en seco. Bogotá: Ministerio de Agricultura y Desarrollo Rural.

SIC. (2025), Resolución No. 65722 de 2025: Autorización de acuerdo en aplicación del parágrafo único del artículo 1 de la Ley 155 de 1959. Bogotá: Superintendencia de Industria y Comercio.

Note: References cited in both the main text and this Supplement (e.g., ICA, 2022; MADR, 2025a; MADR, 2026b; UPME et al., 2010; UPRA, 2020; Durán et al., 2021) appear in full in the main reference list.

S7. BY-MILL MASS–ENERGY BALANCE (CENTRAL SCENARIO)

Referenced from Section 4.4. The table below reports the full by-mill balance underlying the central estimate. The node-level electricity column is shown graphically in Figure III(b) of the main text.

Table S7: Estimated husk generation and gross technical electricity potential by mill (central scenario)

Mill	Regime	Green paddy (t)	Husk gen. (t)	Avail. dry husk (t)	Primary (TJ)	Elec. (MWh/yr)
ORF S.A. – Pore	Gravity	67,654	12,502	5,626	79.3	4,407
Unión de Arroceros	Gravity	41,475	7,665	3,449	48.6	2,702
Diana Corporación	Gravity	37,382	6,908	3,109	43.8	2,435
Agroindustrial Sonora	Gravity	35,149	6,495	2,923	41.2	2,290
Granos y Cereales	Gravity	31,807	5,878	2,645	37.3	2,072
ORF S.A. – Villanueva	Gravity	30,743	5,681	2,557	36.0	2,003
Molinos El Yopal	Gravity	30,240	5,588	2,515	35.5	1,970
Arrocera La Esmeralda	Gravity	28,897	5,340	2,403	33.9	1,882
Arroz Barichara	Gravity	25,115	4,641	2,089	29.4	1,636
Molino Casanare	Gravity	20,735	3,832	1,724	24.3	1,351
Fedearroz – Pore	Capacity	24,000	4,435	1,996	28.1	1,563
TOTAL		373,197	68,965	31,036	437.4	24,311

The “available dry-husk equivalent” column already incorporates the availability factor **A_f** and the moisture correction (1−MC). Totals were computed from unrounded values and may differ slightly from the sum of displayed rows.

The “available dry-husk equivalent” column already incorporates the availability factor **A_f** and the moisture correction (1−MC). Totals were computed from unrounded values and may differ slightly from the sum of displayed rows.

S8. EXTENDED DISCUSSION

Referenced from Section 5.1. This section provides the detailed level-by-level interpretation, the full scenario analysis, and the extended comparison with previous studies, condensed in the main text for length.

S8.1. Level-by-level interpretation

The four-level chain matters because each level answers a different question, and collapsing them produces a category error. The first level identifies residue embodied in Casanare's paddy production but does not indicate where that residue is physically generated. The second level introduces the milling boundary, and the contraction it produces (Figure II) is driven mainly by the estimated location of processing rather than by any physical loss of biomass: paddy assigned to mills outside the modelled network still generates husk, but not at the facilities available for regional energy planning. This is the central contribution of the allocation stage — agricultural origin and agro-industrial residue location are related but not interchangeable.

The third level separates two mechanisms that are frequently conflated. The availability factor accounts for competing uses, internal energy consumption and other commitments, whereas the moisture correction converts available material to the dry basis required for the energy calculation. Treating water removal as a competing use, or assuming that every tonne generated is uncommitted, would misstate the resource in opposite directions. The fourth level applies a technological conversion loss and yields a comparable technical potential under a defined gasification pathway — not a plant design, a net export estimate, or a forecast of delivered electricity. The full-local-processing counterfactual shows why the processing boundary is consequential: under otherwise unchanged parameters, the central estimate captures approximately one third of the electricity associated with processing all departmental paddy at Casanare nodes.

S8.2. Scenario effects

Uncertainty is not evenly distributed across the chain, and its sources are of two kinds. The availability factor produces the widest output span, but this reflects the width of the adopted interval rather than any intrinsic elasticity: Kapur et al. (1996) establish that husk can already support parboiling, drying, milling and electricity requirements within mills, yet no source demonstrates that half of Casanare's husk is uncommitted. The central case is an operational regime representing partial internal or competing use, not an observed availability rate. The husk-to-paddy ratio, by contrast, varies within a narrow band and represents variation in milling yield and mass basis rather than uncertainty in conversion performance; because it applies to dry paddy, it must remain separate from both the green-to-dry conversion and the husk-moisture adjustment.

The heating-value, moisture and efficiency scenarios affect conversion rather than territorial distribution, yielding a specific electricity range of approximately 733 to 1,125 kWh per tonne of dry husk. This is consistent with the literature's emphasis on fuel basis and technology scale (Mansaray and Ghaly, 1997; Wu et al., 2009), and the central value should be read as a reference configuration rather than a universally expected yield. The structurally decisive parameter is the local-processing fraction, because it determines how much of the departmental base enters the modelled network. Unlike the material properties, lambda is not a physical constant: it summarises unobserved commercial flows, cross-departmental processing and inventory coverage. Calibration against one mill makes the central scenario locally grounded but does not convert lambda into an observed departmental share.

S8.3. Extended comparison with previous studies

Three groups of antecedents situate the present results. Aggregate residual-biomass assessments establish the declining sequence observed here: Chauhan (2010) showed that power potential falls when generated biomass is progressively adjusted for existing uses and surplus availability, and Kongchouy et al. (2021) obtained proportional increases when raising collection factors in a national multi-crop GIS assessment — behaviour consistent with the linear role of the availability factor in the Casanare chain. The present study extends that logic to a point-source residue by inserting a milling-location stage before availability and conversion, because husk is generated where paddy is processed rather than where it is harvested. Absolute potentials are not directly comparable across these studies, since they differ in crop coverage, spatial scale and constraint sets; the relevant agreement lies in distinguishing a gross residue inventory from an availability-adjusted energy resource.

Mill-centred assessments provide the second comparison. Kapur et al. (1996) analysed rice-husk electricity within mills and emphasised the interaction between residue availability and internal process demand, a distinction the present results support at a larger spatial scale. Ejiofor et al. (2020) reported a 1.52-MW off-grid gasification system, placing their case in the same broad scale range as the mean output associated with the central estimate here; their study is nevertheless a load-matched design for one locality, whereas the present result aggregates model-implied supply across eleven nodes and reports gross technical potential. Comparison should therefore remain at the level of application scale rather than a per-tonne benchmark.

Colombian and decentralised-processing studies form the third group. Lenis Rodas et al. (2022) demonstrate that rice husk can be gasified in compact mills and identify operating conditions suitable for internal-combustion engines, supporting the selected conversion pathway without estimating a departmental resource or allocating paddy among mills. Thengane et al. (2020) suggest that processing near mills can reduce transport burdens, though their techno-economic and life-cycle conclusions cannot be transferred without mill-specific costs, auxiliary loads and product markets. The present estimate should thus be read as a territorial extension of a technically demonstrated pathway, not as evidence that the same performance has been validated at every Casanare mill.